Published in final edited form as:
Dev Cell. 2011 December 13; 21(6): 1038–1050. doi:10.1016/j.devcel.2011.10.023.

A PLCβ/PI3Kγ-GSK3 signaling pathway regulates cofilin phosphatase slingshot2 and neutrophil polarization and chemotaxis

Wenwen Tang[1,*], **Yong Zhang**[1,*], **Wenwen Xu**[1,*], **T. Kendall Harden**[2], **John Sondek**[2], **Le Sun**[3], **Lin Li**[4], and **Dianqing Wu**[1]

[1]Department of Pharmacology and Vascular Biology and Therapeutic Program, Yale University, School of Medicine, New Haven, CT 06520

[2]Department of Pharmacology, University of North Carolina School of Medicine, Chapel Hill, NC 27599

[3]AbMax, Beijing 100085, China

[4]Shanghai Institute of Biochemistry and Cell Biology, Shanghai, China

SUMMARY

Neutrophils, in response to a chemoattractant gradient, undergo dynamic F actin remodeling, a process important for their directional migration or chemotaxis. However, signaling mechanisms for chemoattractants to regulate the process are incompletely understood. Here, we characterized chemoattractant-activated signaling mechanisms that regulate cofilin dephosphorylation and actin cytoskeleton reorganization and are critical for neutrophil polarization and chemotaxis. In neutrophils, chemoattractants induced phosphorylation and inhibition of GSK3 via both PLCβ-PKC and PI3Kγ-AKT pathways, leading to the attenuation of GSK3-mediated phosphorylation and inhibition of the cofilin phosphatase slingshot2 and an increase in dephosphorylated, active cofilin. The relative contribution of this GSK3-mediated pathway to neutrophil chemotaxis regulation depended on neutrophil polarity preset by integrin-induced polarization of PIP5K1C. Therefore, our study characterizes a signaling mechanism for chemoattractant-induced actin cytoskeleton remodeling and elucidates its context-dependent role in regulating neutrophil polarization and chemotaxis.

Keywords

Neutrophil; Chemotaxis; polarization; Chemoattractant signaling; Slingshot; PLC; GSK3

Introduction

Chemotaxis is a process in which a cell migrates following a gradient of a chemoattractant and plays an important role in embryonic development, wound healing, tumor metastasis,

Correspondence to: Dianqing Wu.

*These authors contributed equally

and various aspects of leukocyte biology including leukocyte infiltration, recruitment, trafficking, and homing. Neutrophils, a type of leukocytes, are an excellent system for studying the basic mechanisms underlying chemotaxis. They are the most motile cells in higher organisms and can efficiently interpret and chemotax under a shallow chemoattractant gradient. Circulating neutrophils are non-polarized. Upon stimulation, they polarize by forming the leading edge or the "front" that is rich in lamellar filamentous actin (F-actin) and the uropod (the "back") that is rich in actomyosin filaments. When a chemoattractant gradient is present, the cell can sense and align its front-back polarity with the chemoattractant gradient and migrate directionally up the gradient. Therefore, cell polarization provides a link between the two other basic characteristics of chemotaxis---directionality (the ability to follow the gradient) and locomotion (or motility). The questions have been how chemoattractants and their gradients regulate the polarization, directionality, and locomotion.

Chemoattractants regulate a wide range of signaling molecules. Among them, phosphatidylinositol 3,4,5-trisphosphate [PtdIns (3,4,5)P_3] has been at the center of chemotaxis research for its localization at the leading edges of chemotaxing *Dictyostelium* cells (Parent et al., 1998). This polarization is attributed to phosphatidylinositol 3-kinase (PI3K) localization at the leading edge and phosphatase and tensin homolog (PTEN) localization at the uropods (Funamoto et al., 2002; Iijima and Devreotes, 2002). Polarized PtdIns (3,4,5)P_3 localization also occurs in neutrophils (Servant et al., 2000). Disruption of the PI3K-PtdIns(3,4,5)P_3 pathway may or may not cause significant defects in neutrophil and *Dictyostelium* chemotaxis depending on the experimental contexts. Together with other signaling pathways being identified for the regulation of *Dictyostelium* and neutrophil chemotaxis, it is now believed that chemotaxis is regulated by multiple signaling pathways [see reviews (Stephens et al., 2008; Afonso and Parent, 2011)]. However, how different signaling pathways interact and contribute to the regulation of chemotaxis, particularly neutrophil chemotaxis, has been understudied.

We and others previously showed that chemoattractants including formyl-Met-Leu-Phe (fMLP) and CXCL2 stimulated PtdIns(3,4,5)P_3 formation via PI3Kγ in mouse neutrophils (Hirsch et al., 2000; Li et al., 2000; Sasaki et al., 2000). One of the mechanisms by which PI3Kγ regulates neutrophil polarization and directionality is to localize the activation of CDC42 and F-actin formation at the leading edge in accordance to the chemoattractant gradients (Li et al., 2003). CDC42 belongs to the Rho family of small GTPases that also include RhoA and Rac (Ridley, 2001; Etienne-Manneville and Hall, 2002). In neutrophils, CDC42 regulates the directionality by directing where F-actin and the leading edge are formed, and Rac promotes F-actin formation in the leading edge (Gu et al., 2003; Li et al., 2003; Srinivasan et al., 2003; Szczur et al., 2009). CDC42 and Rac probably act through the WASP and WAVE complexes. On the other hand, RhoA regulates the formation and contractility of the actomyosin structure at the back via regulating the phosphorylation of myosin light chain (Xu et al., 2003; Shin et al., 2010).

The actin-depolymerizing factor (ADF)/cofilin family of actin-binding proteins plays important roles in actin dynamics and cell migration (Oser and Condeelis, 2009; Bernstein and Bamburg, 2010). Cofilin activity is subjected to various forms of regulations. Among them, its phosphorylation and binding to PtdIns(4,5)P_2 are the best studied for their role in regulating the F-actin-severing activity (van Rheenen et al., 2009; Bernstein and Bamburg, 2010). Cofilin is inactivated by phosphorylation at Ser^3. The LIM (Lin-11/Isl-1/Mec-3) and TES (testicular protein) kinases phosphorylate, whereas slingshot (SSH) and chronophin (CIN) phosphatases dephosphorylate, cofilin at this site (Huang et al., 2006). In neutrophils, chemoattractants induce the dephosphorylation of cofilin (van Rheenen et al., 2009), which appears to depend on Rac (Sun et al., 2007). Because Rac or the other Rho small GTPases

stimulate LIMK/TESKs (Huang et al., 2006, it is unlikely that chemoattractants or Rac stimulate cofilin dephosphorylation via regulating these cofilin kinases.

In this study, we identified a signaling mechanism by which fMLP induces cofilin dephosphorylation via regulating the cofilin phosphatase SSH2. SSH2 is phosphorylated and inhibited by the protein kinase GSK3, which is negatively regulated by fMLP. In neutrophils, fMLP suppresses GSK3 activity by inducing GSK3 phosphorylation through both PLCβ-PKC and PI3Kγ-AKT pathways. Moreover, we demonstrated that this PLCβ/PI3Kγ-GSK3-SSH2 pathway played a role in polarized formation of lamellar F-actin at the leading edge and neutrophil chemotaxis. Furthermore, we investigated the interaction of this GSK3-mediated front signaling pathway with an integrin-regulated back signaling mechanism and revealed how the context may alter the relative significance of this PLC/PI3K pathway in its regulation of neutrophil chemotaxis.

RESULTS

Both PLCβ-PKC and PI3Kγ-AKT signaling pathways are involved in GSK3 phosphorylation in mouse neutrophils

In our attempt to identify additional PtdIns(3,4,5)P_3 effectors in regulating neutrophil chemotaxis, we examined whether PI3Kγ-deficiency affected the phosphorylation of GSK3α at Ser^{21} and GSK3β at Ser^{9}, which are dependent on the PI3K-PtdIns(3,4,5)P_3-Akt signaling axis in many other systems (Downward, 1998). The neutrophil chemoattractant fMLP induced robust GSK3 phosphorylation at both sites, which peaked at ~3 min (Figure S1A). However, PI3Kγ-deficiency, which abrogated Akt phosphorylation at Ser^{473} and Thr^{308} (Figure 1A)(Hirsch et al., 2000; Li et al., 2000; Sasaki et al., 2000), merely reduced GSK3 phosphorylation by around 20% at 3 min of fMLP treatment, although it caused ~60% reduction at 1 min (Figure 1A). The neutrophils lacking PLCβ2/β3 (referred to as PLCβ in this article), which were fortuitously included as a control, also showed reduced GSK3 phosphorylation compared to the wildtype (WT) cells (Figure 1A). PLCβ-deficiency had little effect on fMLP-induced Akt phosphorylations (Figure 1A). Because neutrophils lacking PLCβ2/β3 and PI3Kγ (referred to as “triple KO”) completely failed to responded to fMLP (Figure 1A) or another neutrophil chemoattractant CXCL2 (Figure S1B) in GSK3 phosphorylation, we concluded that both PLCβ and PI3Kγ pathways were required for GSK3 phosphorylation in mouse neutrophils. This conclusion was further supported by the observation that the PI3K inhibitor LY294002 completely abrogated fMLP-induced GSK3 phosphorylation in PLCβ-null neutrophils (Figure S1C).

Consistent with the requirement of PLCβ for PKC activation in mouse neutrophils (Jiang et al., 1997; Li et al., 2000), the PKC inhibitor Ro 31–8220, which inhibits the classic PKC isoforms including PKCα, β and γ, inhibited fMLP-induced GSK3 phosphorylation in WT, but not PLCβ-deficient, neutrophils (Figure S1C). In addition, Ro 31–8220 abrogated GSK3 phosphorylation in PI3Kγ-deficient neutrophils (Figure 1B). The involvement of PKC in GSK3 phosphorylation was further corroborated by the use of phorbol-12-myristate-13-acetate (PMA), a PKC activator. PMA stimulated the phosphorylation of myristoylated alanine-rich C-kinase substrate (MARCKS, a known PKC substrate) and GSK3, which could be inhibited by Ro 31–8220, but not by PLCβ-deficiency or LY294002 (Figure 1C). PMA had little effect on AKT phosphorylation (Figure 1C). Moreover, recombinant PKCα could directly phosphorylate recombinant GSK3β (Figure 1D). These results, together with the fact that the AKT inhibitor (VIII) had similar effects as PI3Kγ-deficiency on GSK3 phosphorylation (Figure 1E), support a conclusion that both PKC and AKT are involved in GSK3 phosphorylation.

Localization of PLCβ2, PKC activation, and GSK3 phosphorylation at the leading edge

PtdIns(3,4,5)P_3 is localized at leading edges of chemotaxing neutrophils and *Dictyostelium* cells. We examined where PLCβ2 is localized in chemotaxing neutrophils. Primary mouse neutrophils expressing GFP-PLCβ2 and a red fluorescent protein tdTomato were stimulated by an fMLP gradient from a micropipette. The localization of GFP-PLCβ2 appeared to be skewed towards the leading edges of chemotaxing neutrophils because the ratios of PLCβ2-GFP to tdTomato became significant higher at the leading edges than those at the uropods after a few of minutes of stimulation (Figure 2A–B, Figure S2A, and Movie S1a). PLCβ2 interacts with and is activated by heterotrimeric G proteins (the Gβγ subunits as well as the α subunits of the Gq family) and the small GTPases including Rac (Harden and Sondek, 2006). Rac shows highly polarized localization at the leading edges of chemotaxing neutrophils (Gu et al., 2003; Srinivasan et al., 2003). Thus, the interaction between Rac and PLCβ2 may have a role in the leading edge localization of PLCβ2. To test the idea, we transfected neutrophils with plasmids encoding tdTomato and a PLCβ2 mutant with a substitution of Ala for Gln^{52} (Q52A). This mutation greatly weakens the interaction of PLCβ2 with Rac (Jezyk et al., 2006; Hicks et al., 2008) and rendered the PLC-β2 mutant unable to exhibit a polarized distribution in chemotaxing neutrophils (Figure 2A–B, Figure S2B, and Movie S1b). This result indicates that PLCβ2's interaction with Rac is critical for its polarized localization at the leading edge.

We next investigated where PKC is activated using an intramolecular FRET (fluorescence resonance energy transfer) probe that has been previously demonstrated to be specific for PKC activation (Violin et al., 2003). There were significantly greater increases in the ratios of 490nm emission to 530 nm emission (Em490/530), which reflects an increase in PKC kinase activity, upon fMLP stimulation in WT cells than the PLCβ-null cells (Figure 2C–D, Figure S2C, and Movie S2a). Importantly, there were greater increases in the Em490/530 ratios at the leading edges than those at the uropods when the cells chemotaxed (Figure 2E). Such increases were absent in PLCβ-null neutrophils (Figure 2C, 2E, S2D and Movie S2b), indicating that the changes observed in the WT cells depend on PLCβ. Consistent with the localization of PKC activation, elevated levels of phosphorylated GSK3 were detected at the leading edges of polarized WT neutrophils by immunostaining (Figure 2F). The triple KO neutrophils, in which no phosphorylated GSK3 was detected by Western analysis (Figure 1A), were used as a negative control for immunostaining (Figure 2F). Thus, we concluded that PLCβ, which is localized to the leading edge in a Rac-dependent manner, stimulated the PKC activity and GSK3 phosphorylation at the leading edge.

Compounded effect of PLCβ and PI3Kγ signaling on neutrophil migration

Knowing that the PLCβ and PI3Kγ signaling is polarized at the leading edge and regulates GSK3 phosphorylation, we wanted to determine their roles in neutrophil chemotaxis. Neutrophils lacking PLCβ2/β3 have been previously examined in a transwell chemotaxis assay, in which the PLC mutant cells showed little defects in response to fMLP or Interleukin 8 (a human ortholog of CXCL2)(Jiang et al., 1997). Neutrophils lacking PI3Kγ have also been evaluated in a number of different chemotaxis assays, and the results varied (discussed in the "Introduction"). The variations may partly be attributed to different surfaces used in the assays, given that integrin signaling had a significant impact on neutrophil polarization (Ferguson et al., 2007; Xu et al., 2010). Therefore, we here examined neutrophil chemotaxis on surfaces coated with poly-lysine, which minimizes integrin signaling, or fibrinogen, which maximizes integrin signaling, in a Dunn chamber assay. We have also introduced some modifications into the Dunn chamber assay as recently described (Xu et al., 2010; Zhang et al., 2010). In this modified assay, the WT and mutant cells were labeled with a yellow cell-tracing dye alternately and assayed simultaneously, and the fMLP gradients were monitored with the FITC dye that diffuses similarly as fMLP. These

modifications help to improve reproducibility and sensitivity of the assay. Using this improved Dunn chamber assay, we found that deficiency in PLCβ, PI3Kγ, or both PLCβ and PI3Kγ did not significantly affect the number of motile neutrophils (Figure S3A–E) or motility (Figure S3F) on the poly-lysine surfaces. These mutant cells, however, show one mild chemotactic defect. They had greater average directional errors than the WT cells with the triple KO cells showing the greatest errors (Figure S3G), suggesting that these mutant cells did not follow the fMLP gradient as well as the WT cells.

When these neutrophils were tested on the fibrinogen surface, the triple KO cells showed a severe chemotactic defect (Figure S3H,I). Approximately 40% of the triple KO neutrophils failed to chemotax in respond to fMLP (Figure 3A) or CXCL2 (Figure 3B). However, the responding cells chemotaxed as fast as the WT cells (Figure 3C), despite with greater directional errors than these cells (Figure 3D),. A previous report had shown that PI3Kγ-deficiency reduced the number chemotaxing neutrophils on fibrinogen (Ferguson et al., 2007). Although in our assay PI3Kγ-deficiency did not cause statistically significant reduction in the chemotaxing cells, there appeared to be a trend for such a reduction (Figure 3A). Together with the lack of a significant effect of PLCβ-deficiency on the number of chemotaxing cells (Figure 3A), we concluded that there was a significant compounded effect on neutrophil chemotactic responses on the fibrinogen surface when both PLCβ and PI3Kγ are depleted.

Because fMLP and CXCL2 stimulate GSK3 phosphorylation and inhibit its activity through PLCβ and PI3Kγ in neutrophils, we tested if pharmacological inhibition of GSK3 would rescue some of the chemotactic defects of the triple KO cells. While the GSK3 inhibitor SB216763 did not significantly affect the number of the WT cells (Figure 3A) or the motility of WT or mutant cells (Figure 3C), it reversed the immotile phenotype of the mutant cells (Figure 3A) in response to fMLP, despite the mutant cells still had a greater directional error than the WT cells (Figure 3D). This incomplete rescue may be due to the incomplete action of the GSK inhibitor or other signaling pathways such as the regulation of PIXα by PI3Kγ (Li et al., 2003). SB216763 was also able to reverse the immotile phenotype in response to CXCL2 (Figure 3B). In addition, another GSK3 inhibitor $LiCl_2$ showed similar effects as SB216763 (data not shown). Therefore, we conclude that GSK3 is involved in PLCβ and PI3Kγ-mediated regulation of neutrophil chemotaxis.

PI3K and PLC-β signaling regulates F-actin polarization in neutrophils

We next wanted to understand why some of the triple KO cells failed to respond to chemoattractants to chemotax. Polarized formation of F-actin upon chemoattractant stimulation plays an important role in chemotaxis. We examined the effect of the triple deficiency on fMLP-induced F-actin polarization. We found that some of the triple KO neutrophils showed broader, less polarized distribution of F-actin staining than the WT cells (Figure 3E) after a quick stimulation by an uniform fMLP. To quantify this difference, we defined a cell with lamellar F-actin staining at the periphery occupying less than 50% of the circumference of the cell as being polarized as described previously (Ferguson et al., 2007) and illustrated in Figure 3E. Fewer of the triple KO neutrophils were “polarized” than the WT cells based on this criterion (Figure 3F). The number of PLCβ or PI3Kγ-null neutrophils exhibiting polarized F actin was between these of WT and the triple KO (Figure 3F). Importantly, GSK3 inhibitors were able to significantly increase the numbers of polarized triple KO cells (Figure 3F). These results suggest that PLCβ/PI3Kγ signaling may regulate actin cytoskeleton reorganization during leading edge formation through their regulation of GSK3.

The significance of the PLCβ/PI3K-mediated front signaling in chemotaxis depends on integrin-induced back signaling

We were intrigued by the dichotomic behaviors of the triple KO neutrophils on fibrinogen, i.e., close to one half of the cells failed to migrate whereas the rest could chemotax almost normally. Fibrinogen can engages Integrins, which can induce polarized localization of PIP5K1C independently of exogenous chemoattractants to specify the initial location of the uropod formed upon chemoattractant stimulation (Xu et al., 2010). Given that neutrophils in the Dunn chamber assay were placed on fibrinogen prior to chemoattractant stimulation, a significant portion of cells might have their polarity preset by integrin signaling as we previously demonstrated (Xu et al., 2010). We thus hypothesized that cells with their preset polarity being aligned against the direction of a chemoattractant gradient might be more dependent on PLCβ/PI3Kγ signaling than those aligned with the gradient to achieve effective F-actin polarization for cell locomotion. To test the hypothesis, we coexpressed GFP-PIP5K1C and Ruby-LifeAct in WT or the triple KO neutrophils. LifeAct-Ruby, a probe with a high affinity for polymerized actin (Riedl et al., 2008), was used to mark the F actin polarization, whereas GFP-PIP5K1C was used to mark the preset polarity by integrin signaling. The cells were placed on fibrinogen to elicit integrin signaling, followed by directional stimulation of fMLP from a micropipette that was placed proximally or distally to polarized GFP-PIP5K1C. Similarly to what we showed previously (Xu et al., 2010), a majority of the WT cells (9 out fo 10) responded, as the one shown in Figure 4A, to form singular F-actin rich leading edges towards the micropipettes when the micropipette was placed distally to polarized GFP-PIP5K1C, i.e., cells were stimulated by fMLP gradients aligned with the preset polarity. When the micropipette was placed proximally to polarized GFP-PIP5K1C, most of the WT cells (8 of 10) were able to eventually form their leading edges toward the micropipette even though LifeAct-Ruby or F actin initially was polarized away from the micropipette (Figure 4B).

Eight of ten triple KO neutrophils coexpressing GFP-PIP5K1C and Ruby-LifeAct behaved like the WT cells when they were stimulated distally to GFP-PIP5K1C (Fig. 4C, Movie S3). However, a majority of the triple KO cells (9 out of 10), when they were stimulated proximally to GFP-PIP5K1C, behaved like the one shown in Figure 4D and Movie S4 and were unable to polarize or chemotax. These cells were not dead, and they often formed more than one F actin-rich pseudopods, which frequently pointed at different direction as the cell shown in Fig. 4D. We then subjected the immotile cells to the treatment of the GSK3 inhibitor $LiCl_2$ (we were unable to use SB216763 in this case due to its high autofluorescence), which enabled six of the nine immotile cells to polarize their F actin to form leading edges and chemotax. Three out of these six cells as the one shown in Figure 4E and Movie S5 were able to eventually polarize and migrate towards the pipette. PLCβ or PI3Kγ-null neutrophils behaved similarly to the WT cells in this test (Figure S4A–D). We also examined cells placed on poly-lysine in which PIP5K1C was not polarized prior to fMLP stimulation. FMLP induced F actin and PIP5K1C polarization in WT and triple KO cells (4 cells out of each genotype, one representative is shown in Figure S4E). Therefore, these results together indicate that the PLCβ/PI3K-GSK3 pathway plays a role in F-actin polarization and leading edge formation. In addition, these results also indicate that the significance of this PLCβ/PI3K-GSK pathway in regulating neutrophil chemotaxis depends on the integrin-induced polarization signal.

GSK3 regulates cofilin phosphorylation

Knowing that GSK3 plays a role in regulation of actin cytoskeleton reorganization, the next question is how GSK3 regulates the reorganization. GSK3 is constitutively active, and phosphorylation at Ser^9 of GSK3β or Ser^{21} of GSK3α upon chemoattractant stimulation leads to suppression of their kinase activity. Therefore, we hypothesized that potential GSK3

downstream targets should be hyperphosphorylated in the absence of a GSK3 inhibitor and may become hypophosphorylated in its presence. Thus, we prepared a set of neutrophil cell extracts from cells treated with or without SB216763. The samples were digested, labeled with the iTRAQ tags, enriched for phosphorylated peptides by TiO_2-affinity chromatography, and subjected to LC-MS-MS and quantitative proteomic analysis. We found that phosphorylation of cofilin at Ser^3 was reduced by SB216763 treatment (Figure S5A). We subsequently confirmed the change in cofilin Ser^3 phosphorylation using a phospho-specific antibody. SB216763, LiCl (Figure 5A), fMLP (Figure 5B) or CXCL2 (Figure S5B) suppressed cofilin phosphorylation in neutrophils. In addition, PLCβ- or PI3Kγ-deficiency reduced, whereas the triple deficiency almost completely abrogated, fMLP-induced inhibition of cofilin phosphorylation (Figure 5B). Moreover, the AKT inhibitor VIII was able to abrogate fMLP-induced dephosphorylation of cofilin in PLCβ-null neutrophils (Figure S5C), further corroborating the conclusion that both PI3Kγ-AKT and PLCβ pathways are responsible for cofilin dephosphorylation. Furthermore, overexpression of an active GSK3β containing a substitution of Ser^9 for Ala, but not the kinase dead mutant, in HEK293T cells could induce cofilin phosphorylation at Ser^3 (Figure 5C). These results demonstrate that fMLP may regulate cofilin phosphorylation via PLCβ/PI3Kγ-regulated GSK3.

We also examined the localization of cofilin and phosphorylated cofilin in neutrophils after fMLP stimulation using specific antibodies. We detected increased cofilin staining at the leading edges of the WT cells, but not the triple KO cells (Figure S5D, E). Because phosphorylated cofilin appeared to be distributed evenly in both WT and triple KO cells (Figure S5F), the elevated total cofilin staining at the leading edges of the WT cells may largely be composed of unphosphorylated cofilin.

GSK3 regulates SSH2

To elucidate the mechanism for GSK3 to regulate cofilin phosphorylation, we first tested if GSK3 could directly phosphorylate cofilin. Recombinant cofilin protein was prepared from a bacterial expression system and used in an *in vitro* kinase assay with recombinant GSK3β. No phosphorylation of cofilin was detected (Figure S6A). However, recombinant GSK3β readily phosphorylated immunoprecipitated full-length cofilin phosphatase SSH2 or a recombinant SSH2 fragment encompassing the N-terminal 460 amino acids (Figure S6B,C). SSH2 was so chosen because its mRNA content is more than ten times higher than that of SSH1, SSH3 or chronophin based on our quantitative gene expression analysis (data not shown). In addition, expression of GSK3β, but not its kinase dead mutant, was able to inhibit SSH2-mediated dephosphorylation of cofilin (Figure S6D). These results together indicate that GSK3β is capable of phosphorylating SSH2 and regulating its phosphatase activity.

Bioinformatic analyses using the ScanSite predicted that the N-terminal 124 amino acids of SSH2 contain multiple potential GSK3 phosphorylation sites. We generated an SSH2 mutant lacking these 124 amino acids (SSH2ΔN, Figure S6E). Although this mutant was capable of dephosphorylating cofilin as efficiently as the WT SSH2 (Compare Lanes 3 & 5 of Figure 6A), GSK3β failed to inhibit SSH2ΔN-mediated dephosphorylation of cofilin (Figure 6A), suggesting that this N-terminal SSH2 sequence may harbor the GSK3 phosphorylation sites for GSK3 to regulate the SSH2 activity. We subsequently generated additional N-terminal deletion mutants (Fig. S6E) and found that deletion of the first 40 amino acids, but not the first 17 amino acids, disabled the regulation of the phosphatase activity by GSK3β (Figure 6A). This hence narrowed the possible GSK3 regulation sites on SSH2 down to Residues 18–40. We then generated a number of point mutations. Single substitution for Ser^{21} or Ser^{32} or double substitution for Ser^{21}/Ser^{25} or Ser^{32}/Ser^{35} for Ala had little or weak effects on GSK3-mediated regulation of SSH2 phosphatase activity

(Figure 6B, S6F). However, substitution for all of these four Ser residues resulted in a mutant (SSH2-S4A) that could not be inhibited by GSK3β in the cofilin dephosphorylation assay (Figure 6B). Consistent with these results, SSH2-S4A was not phosphorylated by GSK3β in an *in vitro* kinase assay (Figure S6G). Moreover, mutation of these four Ser residues to Glu attenuated the phosphatase activity of SSH2 (Figure S6H). All of these results are consistent with the conclusion that GSK3 suppresses the cofilin phosphatase activity of SSH2 through phosphorylation of these Ser residues at the N-terminus of SSH2.

To determine if SSH2 is phosphorylated at any of these four residues in neutrophils, we generated phospho-specific antibodies and were able to obtain two that can recognize phosphorylated Ser^{21} and Ser^{32}, respectively. In a validation experiment, the antibody specific for $pSer^{21}$ was able to detect a band in HEK293T cells expressing the WT SSH2, but not the Ser^{21}-Ala mutant, while the antibody specific for $pSer^{32}$ detected the WT SSH2, but not the Ser^{32}-Ala mutant (Figure S6I). Additionally, coexpression of WT GSK3β, but not its kinase dead mutant, increased the signals (Figure S6I), whereas GSK3 inhibitors reduced the signals (Figure S6J), confirming that phosphorylation of SSH2 at Ser^{21} and Ser^{35} depends on GSK3 in these cells. We detected endogenous SSH2 proteins using these two phospho-specific antibodies. The antibody for $pSer^{21}$ was unable to detect endogenous protein, but the antibody for $pSer^{32}$ was able to detect a band, which could be suppressed by an SSH2 shRNA (Figure 6C). Importantly, fMLP treatment was able to reduce the signals detected by the antibody in the WT neutrophils, but not in the triple KO neutrophils (Figure 6C).

SSH2 regulates cofilin phosphorylation, leading edge formation, and chemotactic directionality in mouse neutrophils

To further corroborate our conclusion that the PLCβ/PI3K-GSK3 signaling pathway regulates neutrophil chemotaxis via its regulation of SSH2, we investigated the role of SSH2 in mouse neutrophil polarization and chemotaxis. We used the method we reported recently (Zhang et al., 2010) to express an SSH2-specific shRNA in primary mouse neutrophils and achieved efficient knockdown of the SSH2 protein contents (Figure 7A). Expression of the *Ssh2* shRNA also impaired fMLP-induced dephosphorylation of cofilin (Figure 7A), suggesting that SSH2 plays a significant role in regulating cofilin phosphorylation in mouse neutrophils.

We then examined the effect of SSH2 knockdown on F-actin polarization. Because cells expressing the *Ssh2* shRNA also expressed YFP, we were able to compare WT and SSH2 shRNA-expressing cells simultaneously (Figure 7B). Expression of the SSH2 shRNA (Figure 7C) resulted in a significant reduction in the number of polarized cells. Expression of YFP alone did not affect the number of polarized cells (Figure S7A–B). Treatment with SB216763, which could reverse the effect of the triple deficiency on F-actin polarization (Figure 3F), did not reverse the effect of SSH2 knockdown (Figure S6C–D), suggesting that SB216763 acted specifically between PLCβ/PI3Kγ and SSH2. In addition, the cells expressing the SSH2 shRNA reduced the number of chemotaxing cells on fibrinogen in the Dunn chamber assay (Figure 7D). We also examined the neutrophil expressing an *Ssh2* shRNA targeting a different *Ssh2* sequence (Figure S7E–G). Thus, these *Ssh2* shRNA expressing neutrophils behaved similarly to the triple KO cells in which GSK3 regulation was compromised, which supports the conclusion that fMLP may regulate polarized F-actin formation and F actin remodeling via a PLCβ/PI3K-GSK3-SSH2-cofilin pathway in mouse neutrophils as depicted in Figure 7E.

DISCUSSION

Previous studies have shown that chemoattractants including fMLP induced cofilin dephosphorylation (Suzuki et al., 1995; Okada et al., 1996; Heyworth et al., 1997), which may involve PI3K and PLC signaling (Okada et al., 1996; Zhan et al., 2003). Our present study revealed how fMLP, via PLC β and PI3Kγ, regulates cofilin dephosphorylation. Our finding that SSH2 is negatively regulated by phosphorylation by GSK3, a constitutively active kinase, is consistent with a previous study showing that dephosphorylation of SSH by a non-specific λ-phosphatase could boost its phosphatase activity (Soosairajah et al., 2005). This GSK3-mediated SSH regulation mechanism may occur in cells beyond neutrophils because PI3K inhibitors can abrogate SSH activation and cofilin dephosphorylation in response to growth factors in cells where the PI3K-AKT pathway is the primary mechanism for phosphorylating GSK3 (Bamburg and Wiggan, 2002; Nishita et al., 2004).

GSK3 has been established for its role in regulation of cell polarity in adherent cells by regulating both microtubule dynamics and organization (Etienne-Manneville and Hall, 2003; Buttrick and Wakefield, 2008). GSK3 was also recently shown to play an important role in Dictyostelium polarization, despite it is regulated differently in Dictyostelium cells from mammalian cells (Kim et al., 2011). Our results in this study have extended the role of GSK3 to the regulation of actin cytoskeleton reorganization. Because microtubules do not appear to play a critical role in rapid neutrophil migration (Xu et al., 2007), the regulation of neutrophil migration by GSK3 may primarily lie in its regulation of SSH2 and cofilin phosphorylation.

There is a growing appreciation for the complexity in chemotaxis regulation. Chemoattractants induce polarization of neutrophils into lamellar F-actin-rich leading edges and contractile actomyosin-containing uropods. Thus, chemoattractants induce dynamic actin cytoskeleton remodeling involving both actin polymerization and depolymerization to form these different types of actin structures with spatial and temporal specifications needed for directional cell migration. Polarized dephosphorylation of cofilin, which depends on both PI3K and PLC in mouse neutrophils, may facilitate polarized formation of lamellar F actin in the leading edge by severing long actin filaments and generating barbed ends. Cofilin dephosphorylation is regulated by signaling mechanisms more than this PLC/PI3K-GSK3 pathway. In neutrophils, RAC, a key regulator for F actin formation in neutrophils, also regulates cofilin dephosphorylation (Sun et al., 2007). Because RAC regulates both PLCβ activity (Hicks et al., 2008) and localization (Figure 2A–B), its regulation of cofilin dephosphorylation may be partially mediated by PLCβ. RAC may also regulate SSH activity via its stimulation of F actin because F actin stimulates SSH activity. This kind of signaling crosstalk and redundancy occur not only to SSH and cofilin dephosphorylation regulation, but also at other levels of signaling cascades. For instance, GSK3 is regulated by the PLC and PI3K pathways, whereas PI3K can also localized CDC42 activation and nucleation of F actin formation in neutrophils. In addition to the crosstalk and redundancy, our results also suggest that the relative significance of one signaling pathway may be context-dependent or depend on the activity of the other signaling pathways in a cell. Specifically, the significance of the PI3Kγ/PLCβ pathway in neutrophil chemotaxis depends on the polarity preset by integrin signaling, which confers neutrophil polarity by polarizing the localization of PIP5K1C and specifying the location of uropods (Xu et al., 2010). The establishment of uropods at one side of a cell induced by integrin signaling may compel the formation of the leading edge at the other side of the cell. If the preset polarity of a cell aligns with the chemoattractant gradient, it would move following the preset polarity, and the PLCβ/PI3K pathway appears to be less important in its polarization and chemotaxis. If the preset polarity aligns against the chemoattractant gradient, the cell may have to rely on these chemoattractant-activated signaling to redirect F actin formation and turn around. We

believe that the crosstalk/redundancy and context-dependency of these signaling pathways may help to understand the variable chemotactic phenotypes reported for disruption of some of the signaling pathways, including the PI3K pathway (Stephens et al., 2008; Afonso and Parent, 2011).

The involvement of PLCβ in cofilin dephosphorylation as revealed by this study may have another advantage. PtdIns(4,5)P_2 binds to dephosphorylated cofilin and inhibits its F-actin severing activity. Thus, PLC activation may not only lead to dephosphorylation of cofilin, but also to a possible reduction in PtdIns(4,5)P_2 contents, which would ensure a full activation of cofilin. Although chemoattractants may only induce transit global reduction in PtdIns(4,5)P_2 contents (Stephens et al., 1993), it is possible that chemoattractants may induce a localized reduction. This possibility will be investigated in future studies.

EXPERIMENTAL PROCEDURES

Reagents and constructs

The wildtype mouse SSH2 expression plasmid and antibody for mouse SSH2 were kindly provided by Tadashi Uemura (Kyoto University, Japan)(Ohta et al., 2003). The GFP-PLC-β2 plasmid was described previously (Hicks et al., 2008). LifeAct-Ruby plasmid is a generous gift from Wedlich-Soldner (Riedl et al., 2008). Plasmid encoding the PKC activity FRET probe, CKAR, was previously described (Violin et al., 2003) and obtained from Addgene. The antibodies specific for phospho-Ser^{21} and Ser^{32} of mouse SSH2 were generated at AbMax (Beijing, China). The SSH2, GSK3 and PLC-β2 mutant plasmids were generated by PCR-based mutagenesis and verified by nucleotide sequencing. The phospho-Ser^{3}-cofilin, cofilin, phospho-GSK3, phospho-Ser^{473}-AKT, phospho-Thr^{308}-AKT, AKT, and phospho-MARCK antibodies were obtained from Cell Signaling Technology, whereas the GSK3 antibody was purchased from Santa Cruz. Alexa Fluor 488 and 633 phalloidins were obtained from Invitrogen. SB216763 was from Sigma. LY294002 was obtained from ALEXIS Biochemicals. Formyl-Met-Leu-Phe (fMLP) was purchased from Sigma (St. Louis, MO). PLCβ2/β3-deficient and PI3Kγ-deficient mice have been previously described (Li et al., 2000). The triple KO mice were generated by intercrossing PLCβ2/β3-deficient and PI3Kγ-deficient mice. Recombinant PKCα and AKT1 proteins were from Cell Signaling Technology, whereas the recombinant GSK3β protein was acquired from SignalChem (Richmond, Canada).

Neutrophil preparation, transfection and treatments

Mouse neutrophils were purified from bone marrows as previously described using a discontinuous Percoll density gradient centrifugation (Zhang et al., 2010). Their transient transfection was carried out using the human monocyte nucleofection kit with the Amaxa system as previously described (Xu et al., 2010). The cells were then cultured for 4 hours in the medium supplied with the kit containing 10% FBS and 25 ng/ml recombinant GM-CSF. Before the cells were used for experiments, they were incubated in HBSS containing 0.2% BSA on ice for 1 hour. Neutrophils may be pretreated with the vehicle (HBSS + 0.1% DMSO), LY294002 (30 μM), Ro31-8220 (10 μM), the AKT inhibitor VIII (10 μM), SB216763 (5 μM), LiCl2 (20 mM) 30 minutes or as noted before chemoattractant stimulation as indicated in the figure legends. For uniform stimulation, 1 μM fMLP or 100 ng/ml CXCL2 were used. For micropipette, 10 μM fMLP or 1μg/ml CXCL2 were loaded to the pipettes. Fibrinogen (100 μg/ML) or poly-lysine (1 mg/mL) was used to coat glass cover slips.

In vitro chemotaxis assay with micropipette or a Dunn chamber

For application of a chemoattractant gradient using a micropipette, an Eppendorf Femotip was loaded with 10 μM fMLP, and an fMLP gradient was maintained by applying a pressure to the micropipette using an Eppendorf FemotaJet microinjection system. The tip of the micropipette was placed and attempted to be maintained at 50 μm from targeted cells. Time-lapse image series were acquired at intervals noted in the figure legends. The chemotaxis assay using a Dunn chamber was carried out as previously described (Zicha et al., 1997) with some modifications as detailed in (Xu et al., 2010; Zhang et al., 2010).

Neutrophils staining

Neutrophils were placed onto the coverslips for 15 minutes before stimulation. In some experiments, neutrophils were pretreated with LY294002, SB216763, or LiCl for 30 minutes, and these inhibitors were present throughout the experiment. The cells were then fixed with 4% Para-formaldehyde and permeabilized with 0.1% Triton in PBS. Mounted slides were observed under a confocal microscopy (Leica SP5). Staining of neutrophils with various antibodies was carried out as previously described (Xu et al., 2010).

In vitro Kinase assay

For assaying phosphorylation of GSK3β by AKT1 and PKCα, GST-GSK3β (80 ng, Signal Chem) was incubated with GST-AKT1 (80 ng, Cell Signaling) in a buffer containing 25 mM Tris-HCl (pH 7.5), 5 mM beta-glycerophosphate, 2 mM DTT, 0.1 mM Na3VO4, and 10 mM MgCl2 or PKCα (136 ng, Cell Signaling) in a buffer containing 0.5mg/ml phosphatidylserine, 50ug/ml 1-stearoyl-2-linoleoyl-sn-glycerol, 50ug/ml 1-oleoyl-2-acetyl-sn-glycerol, 0.15% Triton X-100, 1mM DTT, 2mM CaCl2, 20mM MOPS (pH7.2). The kinase assays were initiated by adding 200 uM ATP and carried out at 37 degree for 1 hour. For assaying phosphorylation of SSH2 or its mutants by GSK3β, purified or immunoprecipitated substrates were incubated with recombinant GSK3β (80 ng) in a buffer containing 25 mM Tris-HCl (pH7.5), 5 mM beta-glycerophosphate, 2 mM dithiothreitol, 0.1 mM Na3VO4, 10 mM MgCl2), and [γ-^{32}P]ATP. After 30 minutes incubation at 30 degree, the reaction mixtures were boiled in the SDS sample buffer and subjected to SDS-PAGE. Radioactive samples were detected by a phosphoimager.

Generation of SSH2-knockdown neutrophils

SSH2-knockdown neutrophils were generated in mice received the transplantation of bone marrow cells infected with shSSH2-expressing viruses as previously described (Zhang et al., 2010). Two independent *Ssh2* shRNAs were used. Their target sequences are: sh*Shh2*- 5'-GCCGGACAGATTGAAGATGAAT and shSHH2-2- 5'-CAGTGTTGGTGTGTTACAGAAA. Neutrophils were prepared from these mice eight weeks after transplantation. The use and care of animals were approved by the Institutional Animal Care and Use Committee at Yale University.

FRET imaging and analysis of live neutrophils

Neutrophils transfected with the PKC FRET probe were stimulated with fMLP from a micropipette. A series of time-lapse images were collected at 30-second time interval. To measure Fret, images were acquired for three sets of measurements: (1) CFP fluorescence (425–445 nm excitation, 455 nm LP dichroic filter, 460–500 nm emission filter); (2) FRET fluorescence (425–445 nm excitation, 455 nm LP dichroic filter, 520–550 nm emission filter); and (3) YFP fluorescence (490–510 nm excitation, 515 nm LP dichroic filter,, 520–550 nm emission filter). Cells of interest were selected for similar expression of YFP and CFP detected by their respective filter sets and recorded using both FRET and CFP sets at 30 sec intervals. Normalized Fret intensity values were calculated as the ratio of CFP

fluorescence to FRET fluorescence, which were further normalized to the ratio of the image preceding fMLP stimulation as reference value set to 1.

Highlights

- Both PLCβ and PI3Kγ are involved in GSK3 regulation in mouse neutrophils
- GSK3 inhibits SSH2 and cofilin dephosphorylation
- PLCβ/PI3Kγ has a context-dependent role in neutrophil chemotaxis regulation

Supplementary Material

Refer to Web version on PubMed Central for supplementary material.

REFERENCES

Afonso PV, Parent CA. PI3K and Chemotaxis: A Priming Issue? Science signaling. 2011; 4:e22.

Bamburg JR, Wiggan OP. ADF/cofilin and actin dynamics in disease. Trends in cell biology. 2002; 12:598–605. [PubMed: 12495849]

Bernstein BW, Bamburg JR. ADF/cofilin: a functional node in cell biology. Trends in cell biology. 2010; 20:187–195. [PubMed: 20133134]

Buttrick GJ, Wakefield JG. PI3-K and GSK-3: Akt-ing together with microtubules. Cell Cycle. 2008; 7:2621–2625. [PubMed: 18728390]

Downward J. Mechanisms and consequences of activation of protein kinase B/Akt. Cur Opin in Cell Biol. 1998; 10:262–267.

Etienne-Manneville S, Hall A. Rho GTPases in cell biology. Nature. 2002; 420:629–635. [PubMed: 12478284]

Etienne-Manneville S, Hall A. Cdc42 regulates GSK-3beta and adenomatous polyposis coli to control cell polarity. Nature. 2003; 421:753–756. [PubMed: 12610628]

Ferguson GJ, Milne L, Kulkarni S, Sasaki T, Walker S, Andrews S, Crabbe T, Finan P, Jones G, Jackson S, Camps M, Rommel C, Wymann M, Hirsch E, Hawkins P, Stephens L. PI(3)Kgamma has an important context-dependent role in neutrophil chemokinesis. Nat Cell Biol. 2007; 9:86–91. [PubMed: 17173040]

Funamoto S, Meili R, Lee S, Parry L, Firtel RA. Spatial and temporal regulation of 3-phosphoinositides by PI 3-kinase and PTEN mediates chemotaxis. Cell. 2002; 109:611–623. [PubMed: 12062104]

Gu Y, Filippi MD, Cancelas JA, Siefring JE, Williams EP, Jasti AC, Harris CE, Lee AW, Prabhakar R, Atkinson SJ, Kwiatkowski DJ, Williams DA. Hematopoietic cell regulation by Rac1 and Rac2 guanosine triphosphatases. Science. 2003; 302:445–449. [PubMed: 14564009]

Harden TK, Sondek J. Regulation of phospholipase C isozymes by ras superfamily GTPases. Annu Rev Pharmacol Toxicol. 2006; 46:355–379. [PubMed: 16402909]

Heyworth PG, Robinson JM, Ding J, Ellis BA, Badwey JA. Cofilin undergoes rapid dephosphorylation in stimulated neutrophils and translocates to ruffled membranes enriched in products of the NADPH oxidase complex. Evidence for a novel cycle of phosphorylation and dephosphorylation. Histochem Cell Biol. 1997; 108:221–233. [PubMed: 9342616]

Hicks SN, Jezyk MR, Gershburg S, Seifert JP, Harden TK, Sondek J. General and versatile autoinhibition of PLC isozymes. Mol Cell. 2008; 31:383–394. [PubMed: 18691970]

Hirsch E, Katanaev VL, Garlanda C, Azzolino O, Pirola L, Silengo L, Sozzani S, Mantovani A, Altruda F, Wymann MP. Central role for G protein-coupled phosphoinositide 3-kinase gamma in inflammation. Science. 2000; 287:1049–1053. [PubMed: 10669418]

Huang TY, DerMardirossian C, Bokoch GM. Cofilin phosphatases and regulation of actin dynamics. Curr Opin Cell Biol. 2006; 18:26–31. [PubMed: 16337782]

Iijima M, Devreotes P. Tumor suppressor PTEN mediates sensing of chemoattractant gradients. Cell. 2002; 109:599–610. [PubMed: 12062103]

Jezyk MR, Snyder JT, Gershberg S, Worthylake DK, Harden TK, Sondek J. Crystal structure of Rac1 bound to its effector phospholipase C-beta2. Nat Struct Mol Biol. 2006; 13:1135–1140. [PubMed: 17115053]

Jiang H, Kuang Y, Wu Y, Xie W, Simon MI, Wu D. Roles of phospholipase C beta2 in chemoattractant-elicited responses. Proc Natl Acad Sci U S A. 1997; 94:7971–7975. [PubMed: 9223297]

Kim L, Brzostowski J, Majithia A, Lee NS, McMains V, Kimmel AR. Combinatorial cell-specific regulation of GSK3 directs cell differentiation and polarity in Dictyostelium. Development. 2011; 138:421–430. [PubMed: 21205787]

Li Z, Hannigan M, Mo Z, Liu B, Lu W, Wu Y, Smrcka AV, Wu G, Li L, Liu M, Huang CK, Wu D. Directional sensing requires G beta gamma-mediated PAK1 and PIX alpha-dependent activation of Cdc42. Cell. 2003; 114:215–227. [PubMed: 12887923]

Li Z, Jiang H, Xie W, Zhang Z, Smrcka AV, Wu D. Roles of PLC-beta2 and - beta3 and PI3Kgamma in chemoattractant-mediated signal transduction. Science. 2000; 287:1046–1049. [PubMed: 10669417]

Nishita M, Wang Y, Tomizawa C, Suzuki A, Niwa R, Uemura T, Mizuno K. Phosphoinositide 3-kinase-mediated activation of cofilin phosphatase Slingshot and its role for insulin-induced membrane protrusion. J Biol Chem. 2004; 279:7193–7198. [PubMed: 14645219]

Ohta Y, Kousaka K, Nagata-Ohashi K, Ohashi K, Muramoto A, Shima Y, Niwa R, Uemura T, Mizuno K. Differential activities, subcellular distribution and tissue expression patterns of three members of Slingshot family phosphatases that dephosphorylate cofilin. Genes Cells. 2003; 8:811–824. [PubMed: 14531860]

Okada K, Takano-Ohmuro H, Obinata T, Abe H. Dephosphorylation of cofilin in polymorphonuclear leukocytes derived from peripheral blood. Exp Cell Res. 1996; 227:116–122. [PubMed: 8806458]

Oser M, Condeelis J. The cofilin activity cycle in lamellipodia and invadopodia. J Cell Biochem. 2009; 108:1252–1262. [PubMed: 19862699]

Parent CA, Blacklock BJ, Froehlich WM, Murphy DB, Devreotes PN. G protein signaling events are activated at the leading edge of chemotactic cells. Cell. 1998; 95:81–91. [PubMed: 9778249]

Ridley AJ. Rho GTPases and cell migration. J Cell Sci. 2001; 114:2713–2722. [PubMed: 11683406]

Riedl J, Crevenna AH, Kessenbrock K, Yu JH, Neukirchen D, Bista M, Bradke F, Jenne D, Holak TA, Werb Z, Sixt M, Wedlich-Soldner R. Lifeact: a versatile marker to visualize F-actin. Nat Methods. 2008; 5:605–607. [PubMed: 18536722]

Sasaki T, Irie-Sasaki J, Jones RG, Oliveira-dos-Santos AJ, Stanford WL, Bolon B, Wakeham A, Itie A, Bouchard D, Kozieradzki I, Joza N, Mak TW, Ohashi PS, Suzuki A, Penninger JM. Function of PI3Kgamma in thymocyte development, T cell activation, and neutrophil migration. Science. 2000; 287:1040–1046. [PubMed: 10669416]

Servant G, Weiner OD, Herzmark P, Balla T, Sedat JW, Bourne HR. Polarization of chemoattractant receptor signaling during neutrophil chemotaxis. Science. 2000; 287:1037–1040. [PubMed: 10669415]

Shin ME, He Y, Li D, Na S, Chowdhury F, Poh YC, Collin O, Su P, de Lanerolle P, Schwartz MA, Wang N, Wang F. Spatiotemporal organization, regulation and functions of tractions during neutrophil chemotaxis. Blood. 2010

Soosairajah J, Maiti S, Wiggan O, Sarmiere P, Moussi N, Sarcevic B, Sampath R, Bamburg JR, Bernard O. Interplay between components of a novel LIM kinase-slingshot phosphatase complex regulates cofilin. EMBO J. 2005; 24:473–486. [PubMed: 15660133]

Srinivasan S, Wang F, Glavas S, Ott A, Hofmann F, Aktories K, Kalman D, Bourne HR. Rac and Cdc42 play distinct roles in regulating PI(3,4,5)P3 and polarity during neutrophil chemotaxis. J Cell Biol. 2003; 160:375–385. [PubMed: 12551955]

Stephens L, Jackson TR, Hawkins PT. Activation of phosphatidylinositol 4,5-bisphosphate supply by agonists and non-hydrolysable GTP analogues. Biochem J. 1993; 296(Pt 2):481–488. [PubMed: 8257441]

Stephens L, Milne L, Hawkins P. Moving towards a better understanding of chemotaxis. Curr Biol. 2008; 18:R485–R494. [PubMed: 18522824]

Sun CX, Magalhaes MAO, Glogauer M. Rac1 and Rac2 differentially regulate actin free barbed end formation downstream of the fMLP receptor. J Cell Biol. 2007; 179:239–245. [PubMed: 17954607]

Suzuki K, Yamaguchi T, Tanaka T, Kawanishi T, Nishimaki-Mogami T, Yamamoto K, Tsuji T, Irimura T, Hayakawa T, Takahashi A. Activation induces dephosphorylation of cofilin and its translocation to plasma membranes in neutrophil-like differentiated HL-60 cells. J Biol Chem. 1995; 270:19551–19556. [PubMed: 7642640]

Szczur K, Zheng Y, Filippi MD. The small Rho GTPase Cdc42 regulates neutrophil polarity via CD11b integrin signaling. Blood. 2009; 114:4527–4537. [PubMed: 19752396]

van Rheenen J, Condeelis J, Glogauer M. A common cofilin activity cycle in invasive tumor cells and inflammatory cells. J Cell Sci. 2009; 122:305–311. [PubMed: 19158339]

Violin JD, Zhang J, Tsien RY, Newton AC. A genetically encoded fluorescent reporter reveals oscillatory phosphorylation by protein kinase C. J Cell Biol. 2003; 161:899–909. [PubMed: 12782683]

Weiner OD, Neilsen PO, Prestwich GD, Kirschner MW, Cantley LC, Bourne HR. A PtdInsP(3)- and Rho GTPase-mediated positive feedback loop regulates neutrophil polarity. Nat Cell Biol. 2002; 4:509–513. [PubMed: 12080346]

Xu J, Van Keymeulen A, Wakida NM, Carlton P, Berns MW, Bourne HR. Polarity reveals intrinsic cell chirality. Proc Natl Acad Sci U S A. 2007; 104:9296–9300. [PubMed: 17517645]

Xu J, Wang F, Van Keymeulen A, Herzmark P, Straight A, Kelly K, Takuwa Y, Sugimoto N, Mitchison T, Bourne HR. Divergent signals and cytoskeletal assemblies regulate self-organizing polarity in neutrophils. Cell. 2003; 114:201–214. [PubMed: 12887922]

Xu W, Wang P, Petri B, Zhang Y, Tang W, Sun L, Kress H, Mann T, Shi Y, Kubes P, Wu D. Integrin-induced PIP5K1C kinase polarization regulates neutrophil polarization, directionality, and in vivo infiltration. Immunity. 2010; 33:340–350. [PubMed: 20850356]

Zhan Q, Bamburg JR, Badwey JA. Products of phosphoinositide specific phospholipase C can trigger dephosphorylation of cofilin in chemoattractant stimulated neutrophils. Cell Motil Cytoskeleton. 2003; 54:1–15. [PubMed: 12451591]

Zhang Y, Tang W, Jones MC, Xu W, Halene S, Wu D. Different roles of G protein subunits beta1 and beta2 in neutrophil function revealed by gene expression silencing in primary mouse neutrophils. J Biol Chem. 2010; 285:24805–24814. [PubMed: 20525682]

Zicha D, Dunn G, Jones G. Analyzing chemotaxis using the Dunn direct-viewing chamber. Methods Mol Biol. 1997; 75:449–457. [PubMed: 9276291]

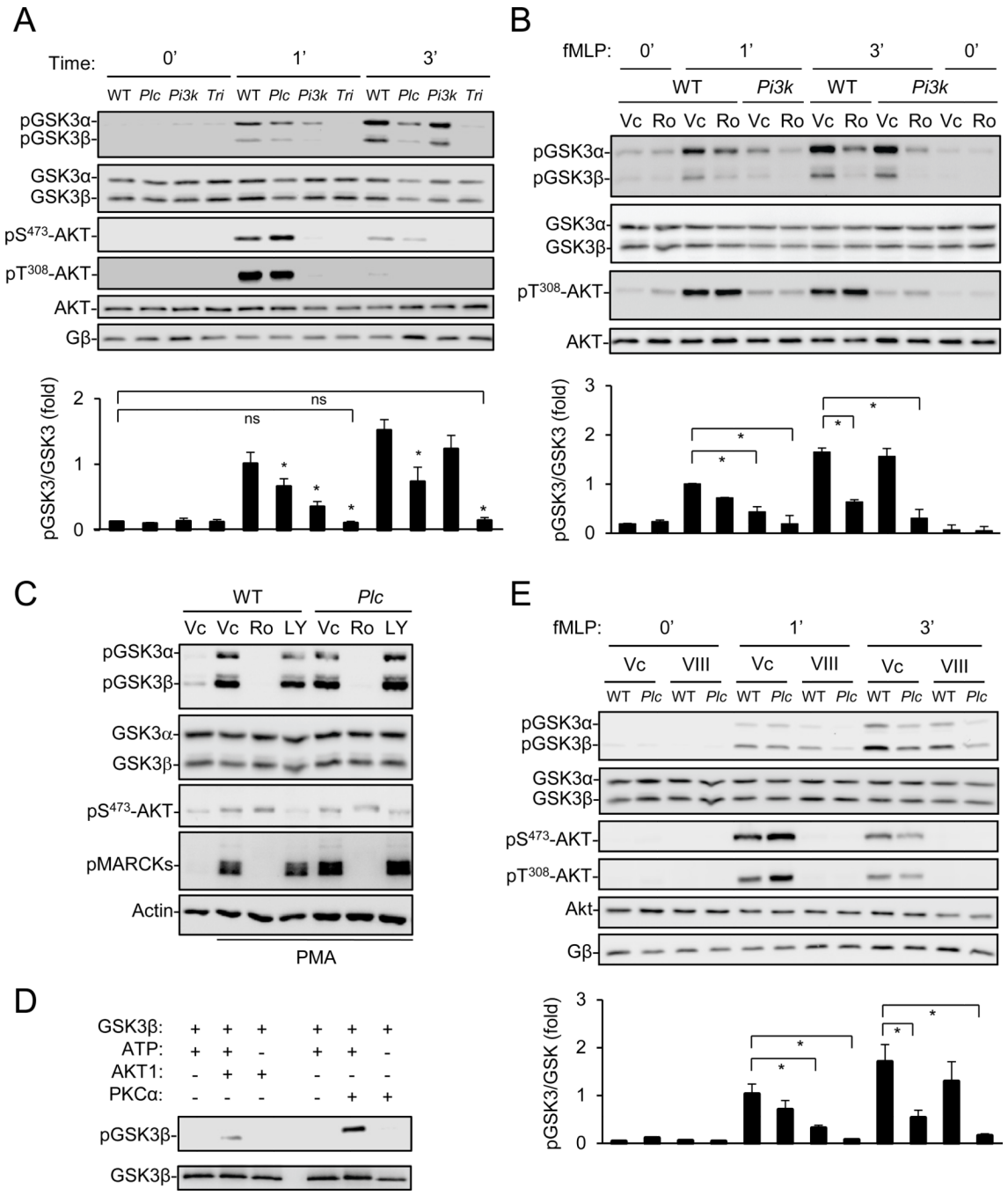

Figure 1. PLCβ-PKC and PI3Kγ-AKT regulate GSK3 phosphorylation in mouse neutrophils

A) Requirement of PLCβ and PI3Kγ signaling for fMLP-induced GSK3 phosphorylation. Neutrophils from wildtype (WT), PLCβ2/β3 (*Plc*), PI3Kγ (*Pi3k*), or PLCβ2/β3;PI3Kγ (*Tri*)-deficient mice were stimulated with fMLP for indicated duration. Data are shown as Mean ± S.E.M. (*, $p<0.05$ vs corresponding WT controls; ns, $p>0.1$; Student's t-Test). See also Fig. S1A–B.

B, E) Pharmacological inhibition of PKC and AKT. WT and mutant neutrophils were pretreated with vehicle control (Vc), Ro 31–8220 (Ro), or the AKT inhibitor VIII, followed by stimulation with fMLP for indicated durations Data quantified from four experiments are shown as Mean ± S.E.M. (*, $p<0.01$; Student's t-Test). See Also Fig. S1C.

C) Stimulation of GSK3 phosphorylation by PMA. Neutrophils were pretreated with LY294002 (LY) or Ro 31–8220 (Ro) for 30 min before stimulation by PMA (1 μM, 8 min). ***D***) Phosphorylation of GSK3β by PKCα and AKT1 in an *in vitro* kinase assay.

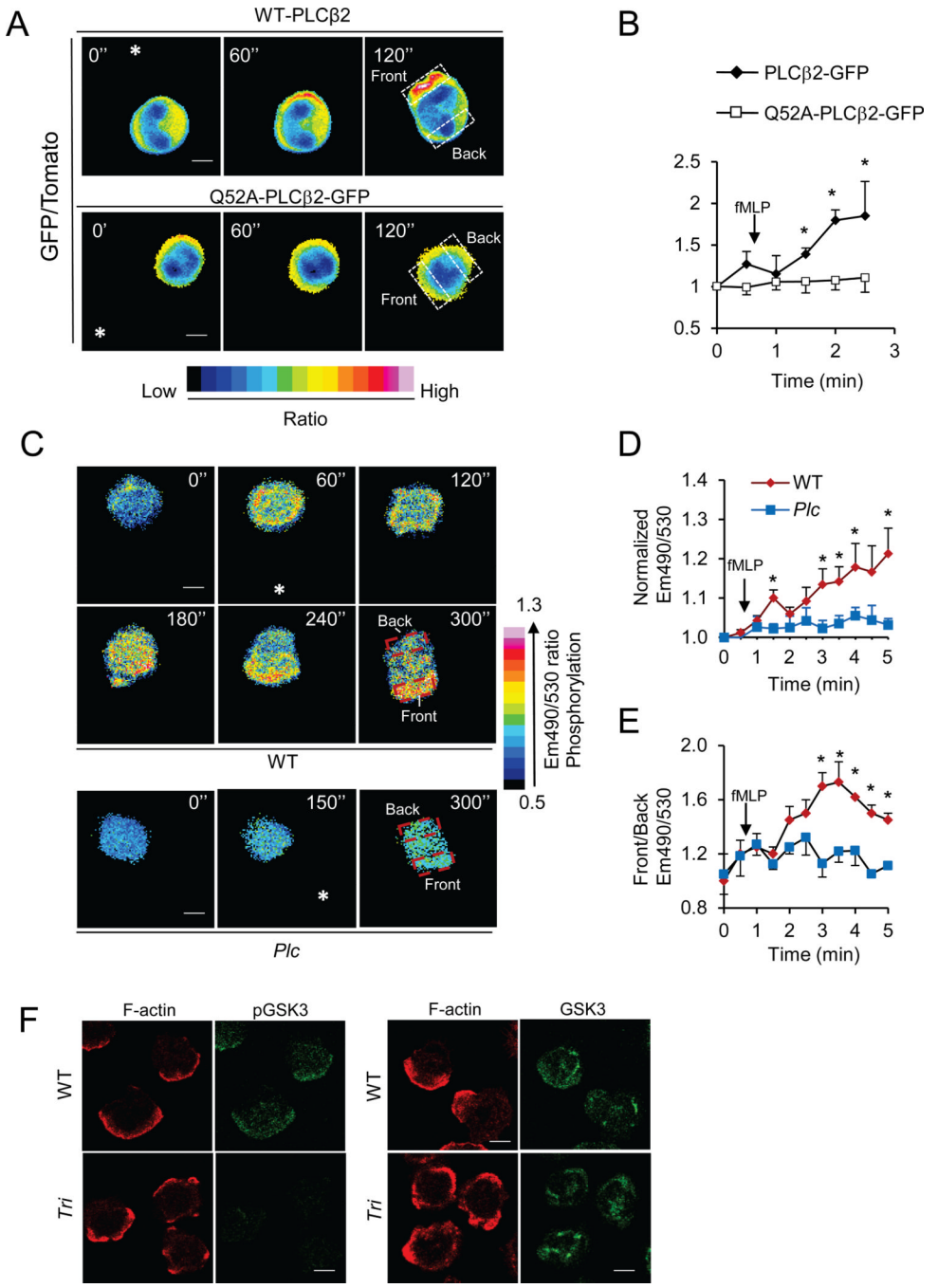

Figure 2. Localization of PLCβ2, PKC activation, and phosphorylated GSK3 in neutrophils

A–B) Leading edge localization of PLCβ2. Wildtype neutrophils expressing tdTomato and PLCβ2-GFP or tdTomato and PLCβ2-Q52A-GFP were stimulated by an fMLP gradient from a micropipette. Images were recorded at 30-second intervals and ratio (GFP/Tomato) images of representative cells are shown. (***A***). The asterisks denote the direction of the micropipette placement. The ratios of front GFP/Tomato ratios to back GFP/Tomato ratios (boxed areas) are plotted in ***B***. Data are shown as Mean ± S.E.M. (*, $p<0.05$ vs Time 0; n=5, Student's t-Test). See also Fig. S2A–B, Movie S1, S2

C–E) Activation of PKC at the leading edge. WT or PLCβ-deficient neutrophils expressing the FRET probe for PKC activity were stimulated with fMLP from a micropipette. Emission

(CFP/FRET) ratio images of representative cells are shown (***C***). Normalized CFP/FRET ratios of the recorded cells (***D***) and ratios of the front emission ratios to the back (boxed areas, ***E***) are plotted. Data are shown as Mean ± S.E.M. (*, $p<0.05$ vs Time 0; n=5, Student's t-Test). See also Fig. S2C–D.

F) Localization of phosphorylated GSK3. Wildtype and triple KO neutrophils were stimulated with fMLP, fixed, and immunostained with a phospho-GSK3 antibody (Green) and Alexa Fluor 633-phalloidin (Red). The cells were examined using a confocal microscope. The scale bars are 4 μm.

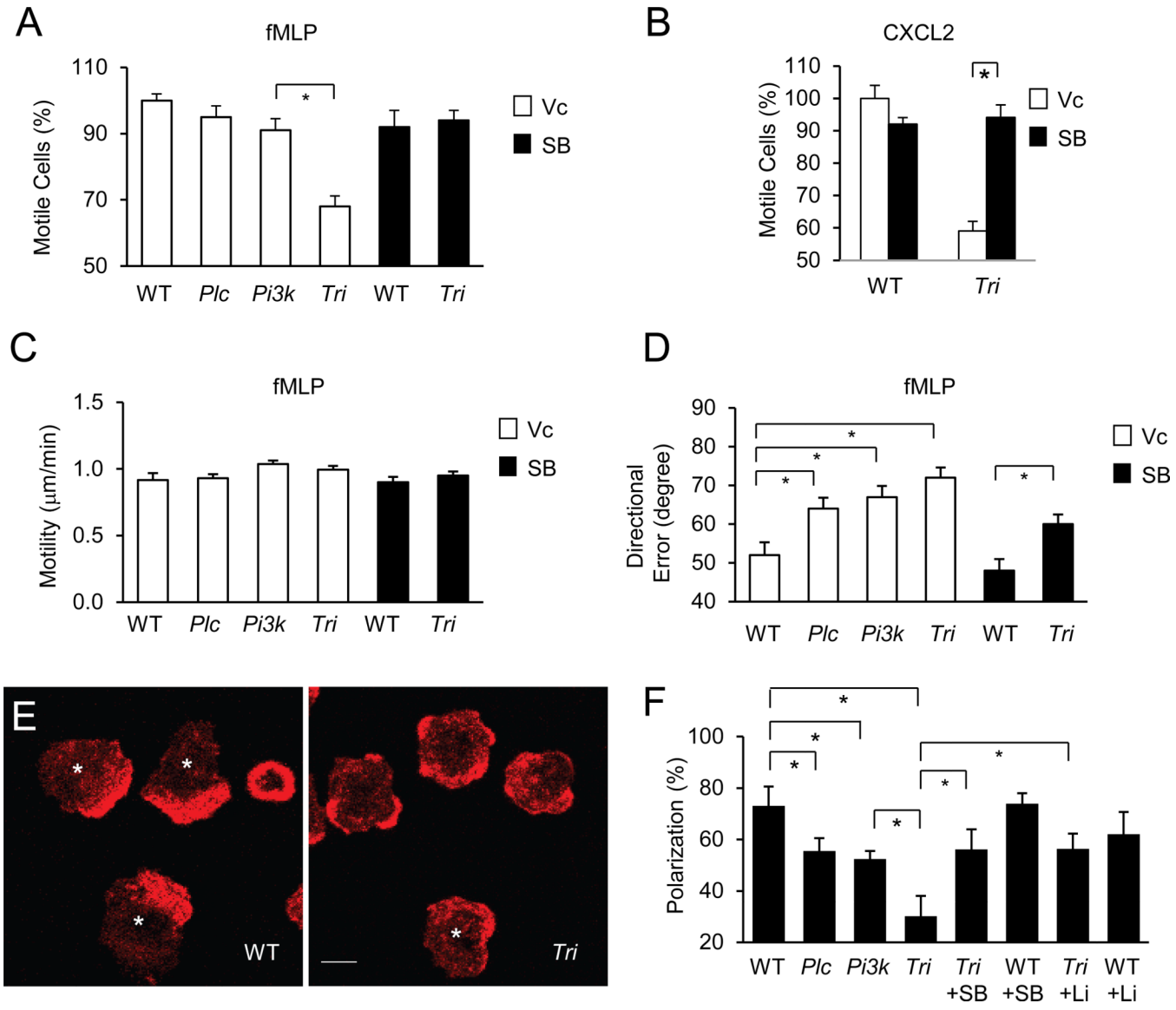

Figure 3. PLCβ/PI3Kγ signaling regulates neutrophil chemotaxis and F actin polarization

A–D) Roles of PLCβ/PI3Kγ signaling in neutrophil chemotaxis on fibrinogen. Chemotaxis of WT and mutant neutrophils pretreated with Vc or SB216763 for 15 minutes was assessed in a Dunn chamber coated with fibrinogen (100 ug/ml) in response to fMLP (***A***, ***C***, **&** ***D***) or CXCL12 (***B***). Percentage of chemotaxing cells relative to WT (85 to 90 % of WT cells were motile in all of these experiments, ***A,B***), motility (***C***), and average directional errors (***D***) are presented as Mean ± S.E.M. (*, $p<0.05$; Student's t-Test). See also Fig. S2.

E,F) Roles of PLCβ/PI3K signaling on F actin polarization. Neutrophils were stimulated with fMLP and stained with Alexa Fluor 633-phalloidin. Representative images of WT or triple KO cells are shown in (***E***). Asterisks indicate cells considered as being polarized in their F-actin distributions. The numbers of cells showing polarized F-actin distribution were quantified from three experiments (more than 50 cells were counted for each condition, ***F***). Data are presented as Mean ± S.E.M. (* $p<0.05$; Student's t-Test).

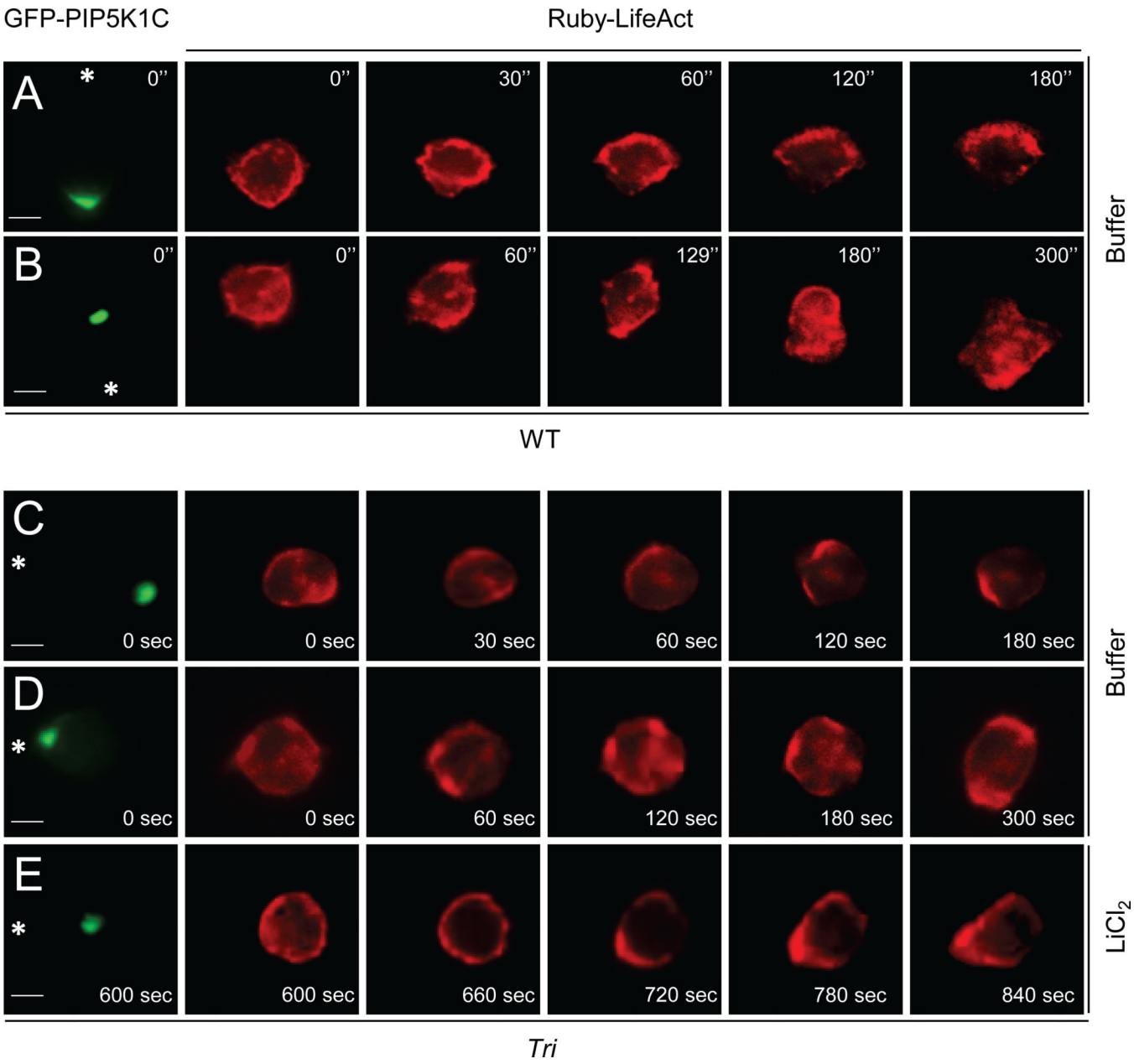

Figure 4. Significance of PLCβ/PI3K signaling in the regulation of chemotaxis depends on the polarity preset by integrin-induced PIP5K1C polarization

WT (***A,B***) or triple KO (***C–E***) neutrophils expressing Ruby-LifeAct and GFP-PIP5K1C were placed on fibrinogen and stimulated by fMLP from a micropipette that was placed distally (***A,C***) or proximally (***B,D,E***) to polarized RFP-PIP5K1C-90. Asterisks denote the direction of the pipette placement. Images were recorded at 30-second intervals and the fMLP was applied at 15 seconds. After 5 minutes of fMLP stimulation, LiCl was added to the cell in ***D***, and the recording was continued (***G***). The scale bars are 4 μm. See also Fig. S4, Movie S3, 4, 5.

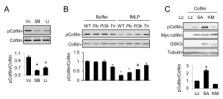

Figure 5. Regulation of cofilin phosphorylation by the PLCβ/PI3Kγ-GSK3 pathway

A) Pharmacological inhibition of GSK3 reduces phosphorylated cofilin contents in WT neutrophils. See also Fig. S5A.

B) Effects of PLCβ, PI3Kγ or PLCβ/PI3Kγ-deficiency on fMLP-induced cofilin dephosphorylation. See also Fig. S5B–F.

C) GSK3 expression stimulates cofilin phosphorylation. HEK293 cells were cotransfected with Myc-tagged cofilin and LacZ (Lz), constitutively active GSK3β (SA), or kinase-dead GSK3β (KM). Cells were analyzed by Western 24 hours after transfection.

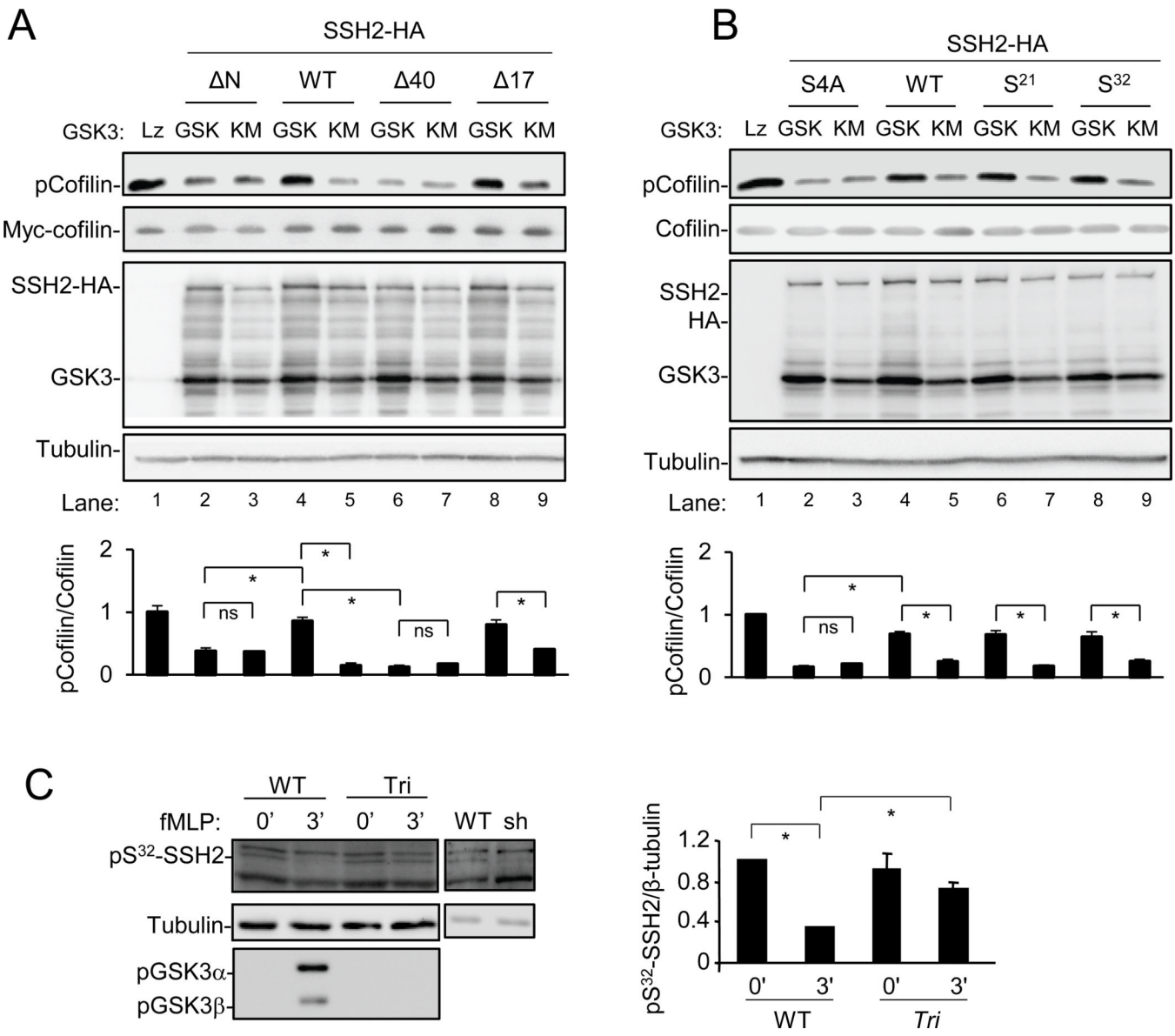

Figure 6. The PLCβ/PI3Kγ-GSK3 pathway regulates SSH2

A,B) GSK3-mediated inhibition of SSH2 depends on SSH2 N-terminal Ser residues. HEK293 cells were co-transfected with Myc-cofilin, wildtype GSK3 (GSK), kinase-dead GSK3 (KM), wildtype SSH2 (WT) or its mutants (ΔN, Δ17, and Δ40 are deletion of N-terminal 125, 17 and 40 amino acids, respectively; S^{21}, Ser^{21} to Ala; S^{32}, Ser^{32} to Ala; S4A, quadruple mutation of Ser^{21}, Ser^{25}, Ser^{32} and Ser^{36} to Ala). See also Fig. S6.

C) PLCβ and PI3Kγ are involved in fMLP-induced dephosphorylation of SSH2 in neutrophils. Neutrophils were stimulated with fMLP for 3 minutes. Endogenous SSH2 phosphorylation was detected by anti-phospho-SSH2-Ser^{32} antibody. Wildtype (WT) and SSH2 knockdown (sh) neutrophil samples were included to indicate the endogenous bands of SSH2.

Immunoblots were quantified from three independent experiments, and data are shown as Mean ± S.E.M. (*, $p<0.01$; ns, $p>0.1$; Student's t-Test).

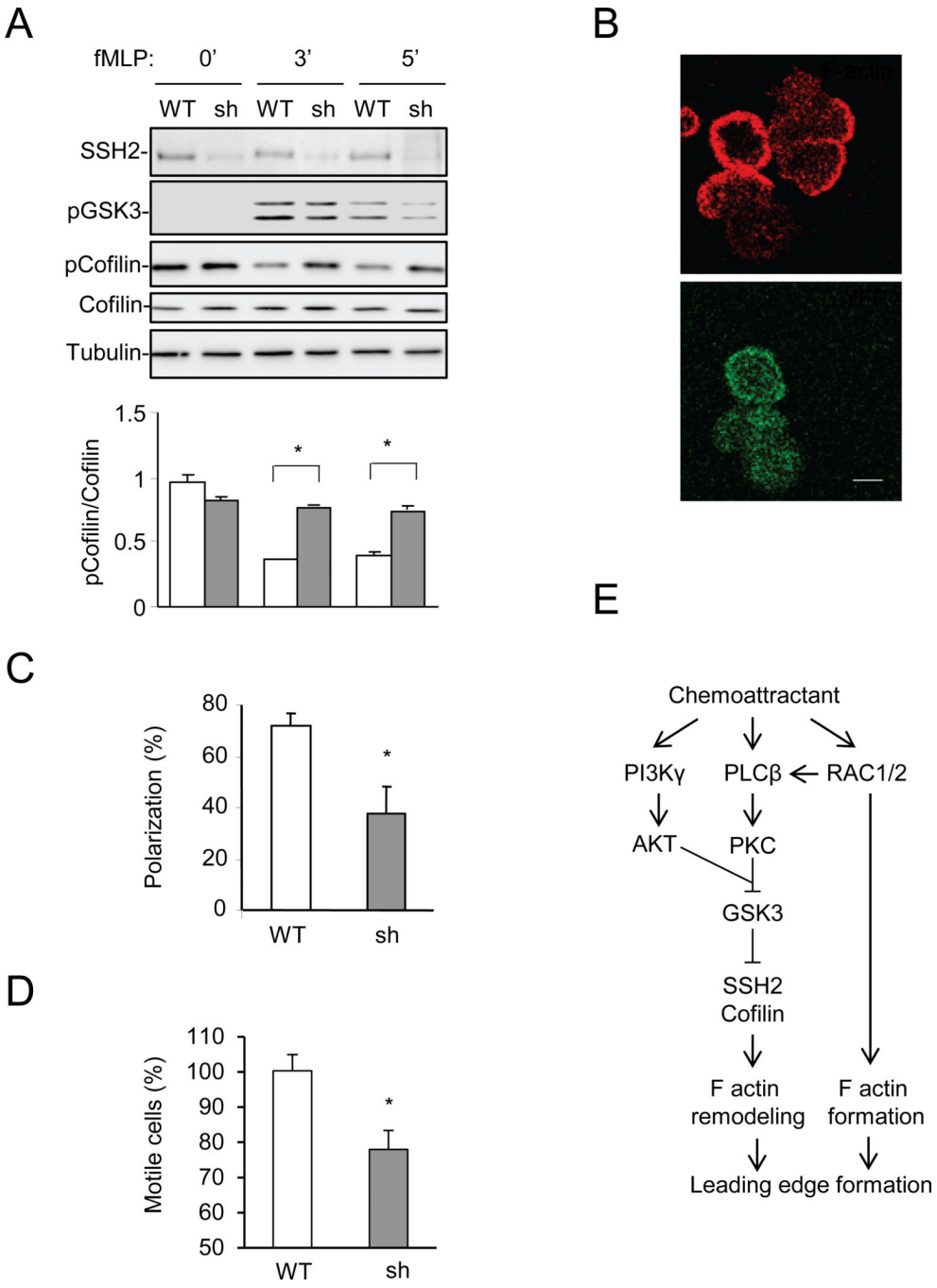

Figure 7. SSH2 regulates neutrophil F actin polarization and chemotaxis

A) SSH2 has a significant role in fMLP-induced cofilin dephosphorylation. Wildtype (WT) or SSH2 knockdown (sh) neutrophils were stimulated with fMLP. Immunoblots were quantified from three independent experiments, and data are shown as Mean ± S.E.M. (*, $p<0.01$; Student's t-Test).

B,C) SSH2 has a significant role in F actin polarization. Wildtype and SSH2 knockdown neutrophils were uniformly stimulated with fMLP for 2 minutes and stained with Alexa Fluor 633-phalloidin. YFP positive cells (Green) are SSH2 knockdown neutrophils. The percentages of cells showing F-actin polarization are shown in ***C*** (total of 136 cells were examined in four separate experiments). The scale bar is 4 μm.

D) SSH2 has a significant role in neutrophil chemotaxis. Chemotaxis of YFP-positive SSH2 knockdown cells and YFP-negative WT cells were evaluated using a Dunn chamber coated with fibrinogen. Data are presented as Mean ± S.E.M. (*, $p<0.05$; Student's t-Test). See also Fig. S7.

E) A model describes the regulation of actin cytoskeleton reorganization by signaling pathways investigated in this study. Both PLCβ and PI3Kγ signaling pathways regulate GSK3 phosphorylation, which suppresses GSK3 kinase activity and relieves GSK3-mediated inhibition of SSH2, leading to cofilin dephosphorylation. While Rac is a key regulator for stimulating actin polymerization, it may also contribute to SSH2 regulation via its regulation of PLCβ.